Available online at www.sciencedirect.com
ScienceDirect
Catalysis Today 130 (2008) 41–49
CATALYSIS TODAY
www.elsevier.com/locate/cattod

Use of the cobalt salt of the heteropolyanion $[Co_2Mo_{10}O_{38}H_4]^{6-}$ for the preparation of CoMo HDS catalysts supported on Al_2O_3, TiO_2 and ZrO_2

Jean Mazurelle [a], Carole Lamonier [a,*], Christine Lancelot [a], Edmond Payen [a], Christophe Pichon [b], Denis Guillaume [b]

[a] *Unité de Catalyse et Chimie du solide, UMR 8181, Université des Sciences et Technologies de Lille, Bâtiment C3, 59655 Villeneuve d'Ascq, France*
[b] *Institut Français du Pétrole, Direction Catalyse et Séparation, IFP-Lyon, BP3, 69390 Vernaison, France*

Available online 17 September 2007

Abstract

Alumina, titania and zirconia supported HDS catalysts have been prepared by incipient wetness impregnation with three solutions respectively based on ammonium heptamolybdate (AHM) and cobalt nitrate, $P_2Mo_5O_{23}^{6-}$ and $Co_2Mo_{10}O_{38}H_4^{6-}$ cobalt salts. Raman spectroscopic analysis of oxidic precursors indicate that at high Mo loadings, MoO_3 and $CoMoO_4$ are present on alumina and zirconia in the AHM based materials whereas TiO_2 appears as the more dispersive support whatever the impregnating solution. The thiophene HDS performances of these catalysts have been evaluated and the results are correlated to the dispersion of the oxomolybdate species in the oxidic precursor and to the promotion of the active phase. This study shows that the $Co_2Mo_{10}O_{38}H_4^{6-}$ cobalt salt is the most efficient precursor that leads to higher dispersion and higher promoting effect.

Keywords: Hydrotreatment catalysis; TiO_2; ZrO_2; Heteropolyanion; EXAFS

1. Introduction

Innovation in the development of hydrotreatment catalysts has been driven by the need to produce clean fuels, based on the pressing requirement for environmental protection. If we consider the Co–Mo–Al_2O_3 system, the active phase consists of well-dispersed MoS_2 nanocrystallites decorated with Co atoms [1]. These active phases are obtained through the sulphidation of an oxidic precursor prepared by incipient wetness impregnation of a γ alumina with an aqueous solution containing the elements to be deposited. Ammonium heptamolybdate (AHM) and cobalt nitrate are generally used for conventional preparation. Many different approaches have been proposed to improve the preparation of these CoMo oxidic precursors like using supports with various acidic properties, additives in the impregnating solution or using new starting materials for the preparation of the impregnating solutions. Particularly the use of different types of heteropolymolybdate, with Keggin, Dawson or Anderson based structures, have been proposed as starting materials for the oxidic precursors preparation [2–5]. Recently Cabello [6] has proposed the use of ammonium salt of $[Co_2Mo_{10}O_{38}H_4^{6-}]$ heteropolyanion (HPA), a dimer structure deriving from the well-known Anderson one. It allows these authors to prepare CoMo-based catalysts that present a higher promoting effect of cobalt in thiophene HDS than the conventional one based on the use of AHM and cobalt nitrate. In the dimer structure, the proximity of cobalt and molybdenum elements can be considered, according to the van Veen's principle [7], as a criterion for obtaining good promoting effect of Co atoms. In a recent work [8] we therefore propose the preparation of oxidic precursors with well-defined Anderson based HPA. In particular the use of cobalt salts allowed us to increase the Co/Mo atomic ratio [9]. For $[Co_2Mo_{10}O_{38}H_4^{6-}](Co_2Mo_{10})$ cobalt salt, a Co/Mo ratio equal to 0.5 is reached, corresponding to the optimum value in the case of conventional preparations. Compared to other Anderson

* Corresponding author. Tel.: +33 320337733; fax: +33 320436561.
E-mail address: carole.lamonier@univ-lille1.fr (C. Lamonier).

0920-5861/$ – see front matter © 2007 Elsevier B.V. All rights reserved.
doi:10.1016/j.cattod.2007.07.008

based HPA and to conventional preparations, this HPA cobalt salt appears as the best starting material for the preparation of HDS catalysts with improved performances [10].

Most of the commercial hydrodesulphurization catalysts contain phosphorus as additive. It has been shown [11] that the addition of phosphorus in conventional impregnating solutions permits to improve the dispersion of the oxomolybdenum species thanks to the formation of the diphosphorepentamolybdenum HPA [$P_2Mo_5O_{23}^{6-}$]. Such molybdo-phosphate based impregnating solutions can be obtained by direct dissolution of molybdenum oxide in a phosphoric acid solution, the cobalt being introduced in the solution as a carbonate salt or as cobalt hydroxide ($Co(OH)_2$) [12,13]. This new method allowed us to prepare impregnating solutions in which the cobalt ions are in the vicinity of the $P_2Mo_5O_{23}^{6-}$ HPA structure and without any foreign counterions such as nitrate or ammonium.

Modification of the alumina carrier or use of other supports has also been proposed to improve the catalytic performances of these CoMo based catalysts. Among the available supports, titania and zirconia appear as the most interesting ones. Moreover many improvements in the preparation of TiO_2 and ZrO_2 were achieved and supports with higher specific area and larger pore diameter are now available. For example, molten salt TiO_2 preparation provides good textural properties with higher specific surface area (120 m^2/g) [14] and Chiyoda Corporation developed mesoporous TiO_2 (120 m^2/g) based on an aqueous precipitation method called ''pH-swing''[15]. Numerous efforts have also been devoted to the preparation of ZrO_2 for hydrotreatment applications. From a catalytic point of view, although titania and zirconia have a small surface area compared to alumina, TiO_2 and ZrO_2 supported MoS_2 catalysts present respectively 3–5 times higher hydrodesulphurization and hydrogenation activities than alumina supported ones with an equivalent Mo loading per nm^2 [16]. To explain this improvement it has been suggested that the active phases supported on TiO_2 (ZrO_2) are uniformly dispersed on the support surface and are better sulphided than on alumina [17]. The electronic effect of the support has also been proposed, Ti^{3+} being considered as a promoter in the decoration position of the MoS_2 slabs [18]. It is also suggested that catalytic activity depends not only on the MoS_2 morphology but also on the orientation of the MoS_2 slabs on the support. Shimada [19] suggests that the surface structure of TiO_2 facilitates the formation of edge-bonded MoS_2 clusters. Considering the active phase, different size and stacking of MoS_2 slabs on supports were proposed to be responsible for better activities on TiO_2 or ZrO_2 [20]. However for promoted system, the synergetic effect of Co and Mo is less efficient on TiO_2 (ZrO_2) than on alumina [16]. In recent theoretical studies, Arrouvel et al. proposed that shorter MoS_2 crystallites are stabilized on TiO_2 [21] and Costa et al. explained that Co promotion could be rather the same on alumina and TiO_2 but the ''quality'' of the CoMoS sites would be inferior on TiO_2 due to a different linkage on the support [22].

This work will tackle the preparation of catalysts supported on alumina, titania and zirconia prepared by incipient wetness impregnation of the support with the three above-mentioned CoMo based impregnating solutions. Various physical techniques will be used to characterize the genesis of the oxidic precursor as well as the dispersion of the active elements. After sulphidation the thiophene HDS performances will be evaluated.

2. Experimental

2.1. Preparation

2.1.1. Preparation of the impregnating solutions

Impregnating solutions were prepared according to three different routes:

(1) Dissolution of AHM and cobalt nitrate in water, the Co/Mo ratio being equal to 0.5. This conventional impregnating solution, which will be named hereafter CoAHM, contained Co^{2+}, $Mo_7O_{24}^{6-}$, NH_4^+ and NO_3^- ions.
(2) Dissolution in water under reflux at 80 °C of a mixture containing MoO_3, H_3PO_4 and $CoCO_3$. The P/Mo and Co/Mo atomic ratios were respectively equal to 2/5 and 0.5. This second impregnating solution, which will be named hereafter CoMoP, contained $P_2Mo_5O_{23}^{6-}$ and Co^{2+} ions.
(3) Dissolution in water of the $Co_3Co_2Mo_{10}O_{38}H_4$ salt (Co/Mo = 0.5).

Preparation of ammonium salt $(NH_4)_6[Co_2Mo_{10}O_{38}H_4]$ is described in the literature [18]. Cobalt salt of the dimer $[Co_2Mo_{10}O_{38}H_4]^{6-}$ heteropolyanion was obtained by cationic exchanges in aqueous solution, $Co_{3/2}PMo_{12}O_{40}$ being the Co precursor for this exchange. This impregnating solution, which will be named hereafter $Co_2Mo_{10}Co$, contained $[Co_2Mo_{10}O_{38}H_4]^{6-}$ and Co^{2+} ions.

2.1.2. Preparation of the oxidic precursors

The characteristics of the three used supports are reported in Table 1. The oxidic precursors were prepared by incipient wetness impregnation of γ alumina, TiO_2 and ZrO_2 extrudates with the three aforementioned impregnating solutions. For a given support three series of solids have been prepared with various amounts of Mo, the Co/Mo ratio being fixed (0.5). The maximum Mo loading depends on the solubility in water of the starting salts [AHM: 1.74 mol Mo per L and $Co_3[Co_2Mo_{10}O_{38}H_4]$: 1.80 mol Mo per L] and principally on the support pore volume. Whatever the series, the Mo loading is expressed as a MoO_3 wt.% and the highest one that can be obtained with the $Co_2Mo_{10}Co$ impregnating solutions is reported in Table 1. The corresponding values of the number of molybdenum atoms per nm^2 (noted dMo) are also reported. After 2 h of maturation, in order to let the species diffuse into the extrudates, the solids were dried under air at 100 °C, and then calcined at 500 °C for 4 h under pure oxygen.

The oxidic precursors were designated according to the nature of the impregnating solution as *X*AHMCoA, *X*CoMoPT, *X*Co_2Mo_{10}CoZ where *X* is the molybdenum loading, A, T or Z corresponding to alumina, titania or zirconia respectively.

Table 1
Supports Characteristics metal loading expressed as MoO_3 (wt.%)

Support	Crystallographic phase	PZC[a]	BET surface area (m^2/g)	Pore volume (cm^3/g)	MoO_3	
					wt.%[b]	dMo[c]
Al_2O_3	Gamma	≈9	200	0.8	16	3.6
TiO_2	Anatase	≈6	100	0.4	10	4.2
ZrO_2	Monoclinic (85%), tetragonal (15%)	≈6	100	0.4	10	4.2

[a] Point of zero charge.
[b] Highest metal loading of the oxidic precursor obtained from $Co_2Mo_{10}Co$ solution by the incipient wetness impregnation method.
[c] Molybdenum atoms nm^{-2}.

Mo loadings have been checked by X-ray fluorescence (Service Central d'Analyses du CNRS, Vernaison-France).

2.2. Characterization techniques

2.2.1. Raman spectroscopy

Raman spectra of the samples, maintained at room temperature, were recorded using a Raman microprobe (Infinity from Jobin-Yvon), equipped with a photodiode array detector. The excitation laser source was the 532 nm line of an Nd-YAG laser, with a wavenumber accuracy of 2 cm^{-1}. The spectra were recorded in the 100–1100 cm^{-1}, however, due to the intense lines of titania or zirconia supports, only the 800–1100 cm^{-1} spectral range characteristic of the Mo–O stretching vibrational modes is presented here.

2.2.2. High-resolution transmission electron microscopy

The high-resolution electron microscopy studies (HREM) were performed on a Tecnai microscope (200 kV). The sample was dispersed in heptane using an ultrasonic device and then deposited on carbon films supported on copper grids.

2.2.3. XAS spectroscopy

Mo and Co K-edge EXAFS (extended X-ray absorption fine structure) measurements were carried out in the Deutches Electronen Synchrotron (DESY, Hamburg) at the EXAFS beamline XI, using synchrotron radiation from the Doris III storage ring, running at 4.5 GeV. The sulphidation was performed directly in the in situ EXAFS cell under a flow of H_2/H_2S (90/10) at 400 °C for 2 h.

The Mo and Co K-edges EXAFS regions of the spectra were extracted and analysed using A. Michalowicz's software packages EXAFS 98 ppc and Round Midnight. The EXAFS spectrum was first transformed from k-space (k^3, Kaiser window 3.7–13.3 $Å^{-1}$ for the Mo K-edge and 2.2–14.9 $Å^{-1}$ for the Co K-edge) to R-space to obtain the radial distribution function (RDF). The EXAFS spectrum for one or several coordination shells was isolated by inverse Fourier transform of the RDF over the appropriate region and fitted using the single scattering EXAFS equation with amplitude and phase functions calculated by FEFF using the interatomic distances deduced from reference compounds.

2.2.4. XPS

XPS experiments were performed using a vacuum generator Escalab 220Xl spectrometer. A monochromatized aluminum source was used for excitation. Binding energy (BE) values were referenced to the binding energy of C 1s (285 eV) and have been given with an accuracy of ±0.1 eV. After their sulphidation under H_2/H_2S (90/10) for 4 h at 673 K, samples were transferred in the spectrometer chamber using a gloves bag in order to avoid any reoxydation.

2.3. Catalytic activity

Catalytic activities for thiophene HDS were measured at atmospheric pressure in a flow-bed reactor packed with 200 mg of catalyst. The oxidic precursors were sulphided at 673 K for 2 h under a flow (100 mL min^{-1}) of H_2S/H_2 mixture (10/90) in the catalytic reactor, then the temperature was cooled down to 573 K. After purification by vacuum distillation, thiophene was introduced in the reactor at constant pressure (50 torr) in a flow of purified hydrogen (20 mL min^{-1}). The reaction products (butane and butene) were analysed by gas chromatography.

3. Results

3.1. Raman analysis of the oxidic precursors after maturation, drying and calcination

3.1.1. Alumina support

Among the supports, alumina is the most studied and numerous results have already been reported in the literature on conventional oxidic precursors prepared with AHM and cobalt nitrate. After maturation, Raman spectra of the AHMCoA with high Mo loading (≥16 MoO_3 wt.%) reveal the presence of precipitated $AlMo_6O_{24}H_6(NH_4)_3$ salt. After calcination and transfer in air, Raman spectra at these high Mo loaded oxidic precursors exhibit the features of bulk oxides as MoO_3 (lines at 995 and 819 cm^{-1}) and $CoMoO_4$ (lines at 940 and 818 cm^{-1}) with those of the well-dispersed polymolybdate phase (broad line centred around 947 cm^{-1}). At lower Mo loadings, only this latter is observed, that is now considered as consisting of well-dispersed $AlMo_6O_{24}H_6^{3-}$ ($AlMo_6$) entities [10]. These entities are formed during the maturation and preserved during the drying step. However, even if they are destroyed upon calcination, they are recovered after transfer in air thanks to the rehydration in wet atmosphere.

When using CoMoP impregnating solution, in agreement with previous results [12,13], the $P_2Mo_5O_{23}^{6-}$ HPA entities are partially preserved on alumina after the drying step whereas after calcination Raman spectra exhibit the features of the

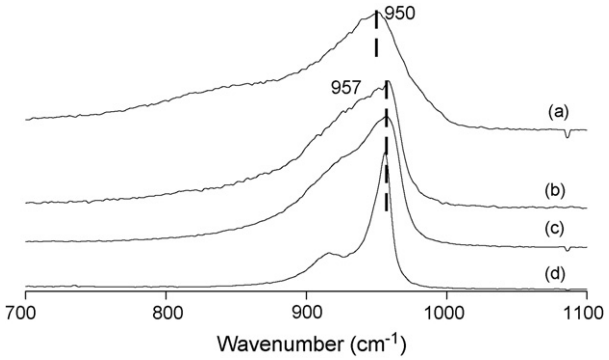

Fig. 1. Raman spectra of Al_2O_3 supported oxidic precursors, $Co_2Mo_{10}CoA$, after calcination (a), after drying (b), after maturation (c), and of $Co_2Mo_{10}Co$ solution (d).

aforementioned well-dispersed polymolybdate phase (main line at 950 cm^{-1}) until a molybdenum loading of 16 wt.%. At higher Mo loadings the presence of $CoMoO_4$ is also observed (spectrum not reported here), which shows the improvement of the dispersion thanks to the absence of ammonium counterions.

Fig. 1 presents the Raman spectra of the $16Co_2Mo_{10}CoA$ oxidic precursor and of the $Co_2Mo_{10}Co$ solution for comparison purpose. After maturation and drying, the line at 957 cm^{-1} indicates the preservation of the $[Co_2Mo_{10}O_{38}H_4]^{6-}$ HPA entities on the alumina support. Moreover, this preservation has been confirmed by XAS experiments performed at the Co K-edge [10]. After calcination, only the well-dispersed polymolybdate species were detected by Raman (Fig. 1(a)), attesting the good dispersion of molybdenum and cobalt even at high Mo loading.

Thus the use of the CoMoP and $Co_2Mo_{10}Co$ impregnating solutions allows us to improve the dispersion.

3.1.2. Titania support

In Fig. 2A are reported the Raman spectra of the calcined oxidic precursors prepared with the CoAHM and CoMoP impregnating solutions. Thanks to the textural properties of the supports the maximum Mo loading (11 MoO_3 wt.%) corresponds to the Mo density of the 16 MoO_3 wt.% alumina based catalyst. Whatever the solid analysed, only a broad line around 955–960 cm^{-1} is observed attesting the presence of a well-dispersed polymolybdate phase.

The Raman spectra of $Co_2Mo_{10}CoT$ oxidic precursors are presented Fig. 2B. The observation of the line at 957 cm^{-1} at the beginning of the maturation is in agreement with the preservation of the Co_2Mo_{10} HPA. However during the maturation an evolution of the Raman spectrum is observed, which shows that the HPA is rapidly destroyed, yielding polymolybdate entities (characterized by a broad line at 950 cm^{-1}) that are maintained after drying and calcination. Whatever the starting impregnating solutions the formation of bulk oxide is not evidenced attesting the good dispersion of the oxomolybdate entities.

3.1.3. Zirconia support

The Raman spectra of AHMCoZ and CoMoPZ oxidic precursors are presented Fig. 3A. Whereas only a broad line centred at 945 cm^{-1} appears on the Raman spectrum of the 10CoMoPZ oxidic precursors, Raman spectrum of 10AHM-CoZ one exhibits also narrow lines at 818, 940 and 995 cm^{-1} which are characteristic of $CoMoO_4$ and MoO_3 oxides. For the preparation of $Co_2Mo_{10}CoZ$ solids a similar evolution of the HPA as with the titania based one is observed (Fig. 3). However the good dispersion is preserved as only the features of well-dispersed polymolybdate phase is evidenced by Raman spectroscopy.

3.2. Characterizations of the sulphided catalysts

All these oxidic precursors have been sulphided and characterized by XPS and EXAFS spectroscopies and HRTEM.

The Fig. 4A and B present respectively the Mo 3d and Co 2p XPS peaks of the supported $Co_2Mo_{10}Co$ based catalysts. XPS analyses show no difference in the position and shape of the Mo 3d and Co 2p peaks. The Mo 3d BEs are 228.9 and 232 eV for respectively the Mo $3d_{5/2}$ and Mo $3d_{3/2}$ components and the Co

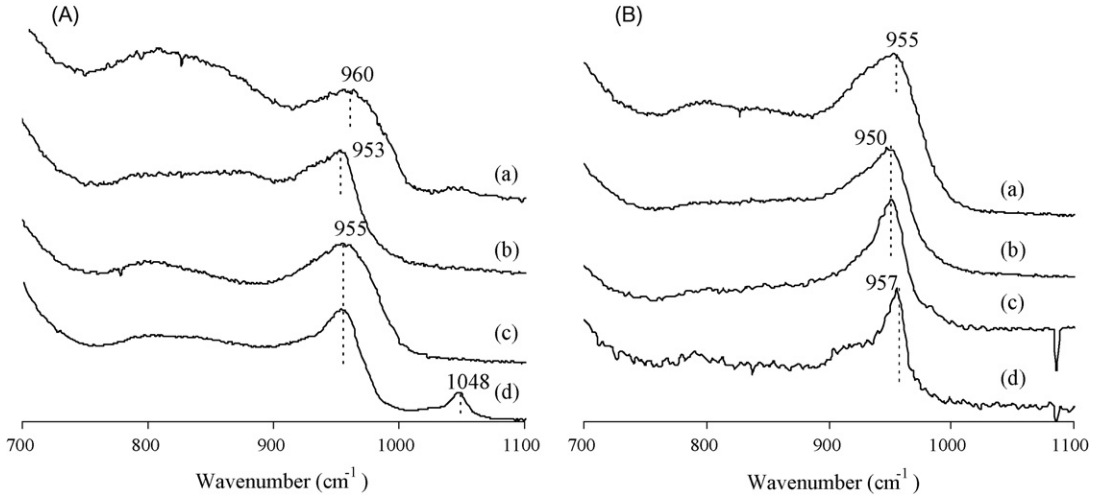

Fig. 2. Raman spectra of TiO_2 supported oxidic precursors, CoMoPT, after calcination A(a), after drying A(b), AHMCOT, after calcination A(c), after drying A(d), $Co_2Mo_{10}CoT$, after calcination B(a), after drying B(b), after maturation B(c), at the beginning of the maturation B(d).

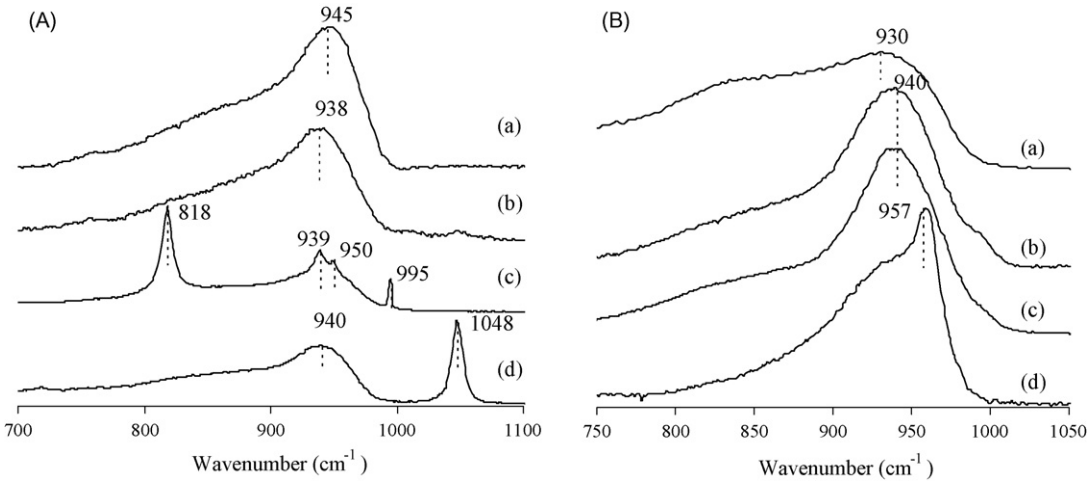

Fig. 3. Raman spectra of ZrO_2 supported oxidic precursors, CoMoPZ, after calcination A(a), after drying A(b), AHMCOZ, after calcination A(c), after drying A(d), $Co_2Mo_{10}CoZ$, after calcination B(a), after drying B(b), after maturation B(c), at the beginning of the maturation B(d).

2p BEs are 778.9 and 793.7 eV for respectively the Co $2p_{3/2}$ and Co $2p_{1/2}$ components. Quite similar results were obtained for the AHMCo and CoMoP based catalysts (spectrum not reported here). In all cases the Mo BEs characterize the presence of MoS_2 entities whereas the binding energy difference E(Co 2p) − E(Mo 3d), equal to 520 eV (±0.2 eV) characterizes cobalt atoms in a decoration position according to the Topsoe's model.

The morphology of the MoS_2 slabs was characterized by HRTEM. The results of the statistic analyses of their length and stacking for the $Co_2Mo_{10}Co$ catalysts are reported in Fig. 5. Differences are observed between the $16Co_2Mo_{10}CoA$, the $10Co_2Mo_{10}CoT$ and $10Co_2Mo_{10}CoZ$ catalysts, these two latter being nearly similar. Whatever the starting impregnating solutions, the highest stacking is observed with the alumina support, whereas the lowest one is observed with the TiO_2 supported catalysts (results not reported here for the CoAHM and CoMoP based catalysts). Eventhrough a higher quantity (20%) of short slabs (<23 Å) is present on $10Co_2Mo_{10}CoT$ and $10Co_2Mo_{10}CoZ$, the average length of the MoS_2 crystallites is similar whatever the support, around 34 Å and corresponds to the average length also observed with the other impregnating solutions.

EXAFS measurements at the Mo K-edge have been performed for $16Co_2Mo_{10}CoA$ and $10Co_2Mo_{10}CoT$. The EXAFS signals and the modulus of the Fourier transform are presented Fig. 6. The refinement is successful as shown in Table 2 where are reported the main parameters of the refinement process, i.e. the number of neighbours N, the distance R between Mo and its neighbours, Debye–Waller factor $\Delta\sigma$, the shift in energy ΔE, and the residue after fitting. The modulus of the Fourier transform presents the coordination shells around the Mo atoms: the first shell contains the contribution of the S neighbours, whereas the second shell contains the contribution of the Mo neighbours. The EXAFS spectra and the FT modulus of the two catalysts are very similar indicating that in both cases the same MoS_2 phase is formed during the activation process; nevertheless the number of Mo neighbours as well as the number of S neighbours appears smaller in the case of TiO_2 supported catalysts. This decrease of the N(Mo–Mo) coordination is then not in relation with the aforementioned particles size on TiO_2 (34 Å as on Al_2O_3). It appears very difficult to estimate the particle size with EXAFS experiments and a theoretical study correlated with EXAFS experiments [23] have shown that the presence of distortions

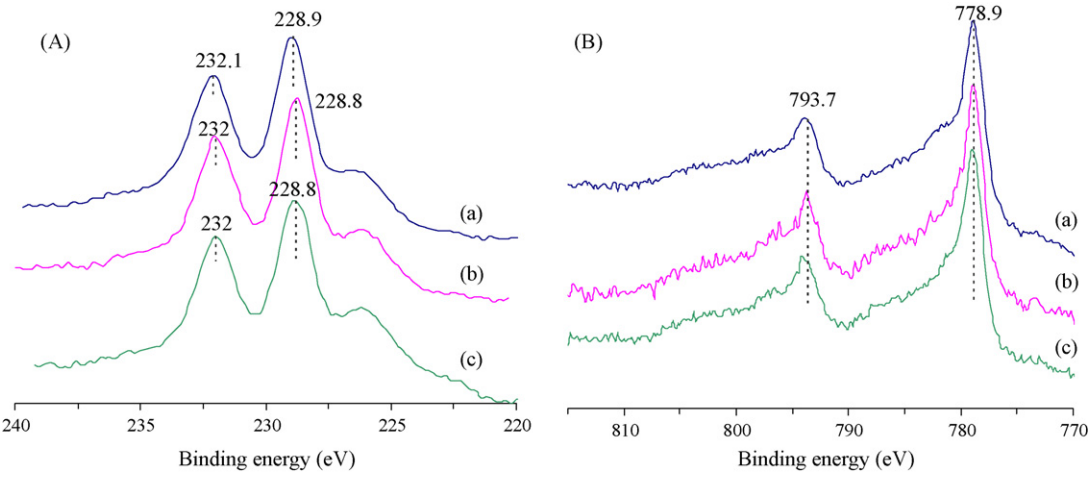

Fig. 4. Mo 3d (A) and Co 2p (B) XPS lines of sulphided $Co_2Mo_{10}Co$ based catalysts supported on Al_2O_3 (a), TiO_2 (b) and ZrO_2 (c).

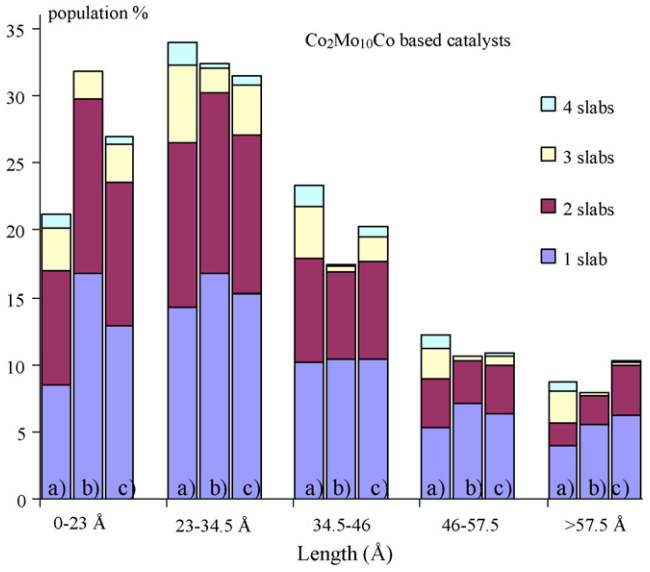

Fig. 5. Statistic analyses (length and stacking) of MoS_2 crystallites from HRTEM pictures of $Co_2Mo_{10}Co$ based catalysts supported on Al_2O_3 (a), TiO_2 (b) and ZrO_2 (c).

(for example sulphur vacancies) influences the calculation of the apparent *N*(Mo–Mo). In situ measurements under various atmospheres have been performed and should help for this determination.

At the Co K-edge, the modulus of the Fourier transform and the EXAFS signals of $16Co_2Mo_{10}CoA$ and $10Co_2Mo_{10}CoT$ are presented in Fig. 7. Similarities in the EXAFS spectra are observed between the two catalysts for the first oscillations, indicating that the cobalt environment on TiO_2 and on Al_2O_3 are quite similar. Changes in the amplitude are better observed on the Fourier Transform that presents two coordination shells at the same uncorrected position (1.4 and 1.8 Å). The two contributions are well resolved whereas one broad peak that should contain more than one contribution are generally observed for such cobalt based sulphided catalysts [24,25]. The

Table 2
Refinements of the Mo K-edge EXAFS signals for $16Co_2Mo_{10}CoA$ and $10Co_2Mo_{10}CoT$ catalysts

	Mo–S		Mo–Mo	
	$16Co_2Mo_{10}CoA$	$10Co_2Mo_{10}CoT$	$16Co_2Mo_{10}CoA$	$10Co_2Mo_{10}CoT$
N	6.49	6.15	2.93	2.6
$\Delta\sigma$	0.01	0.02	0.01	0.02
R	2.42	2.42	3.14	3.15
ΔE	0.0	0.0	0.0	0.0
Residue	0.02	0.03	0.02	0.03

first shell, that is largely emphasized in the case of TiO_2 supported catalyst, is not yet clearly established and could be assigned to Co–O contribution as suggested by the recent literature [26] whereas the second one corresponds to Co–S contributions. However, whatever the solids the formation of Co_9S_8 is not revealed through comparison of Co_9S_8 EXAFS signals reported by Okamoto [27] at the Co K-edge.

3.3. Catalytic results: thiophene hydrodesulphurization

The thiophene conversion versus the molybdenum loading (expressed as MoO_3 wt.%) is reported in Fig. 8 for the nine types of catalysts (three supports and three impregnating solutions). They all exhibit a maximum that is however less apparent in the case of TiO_2 supported catalysts. Whatever the support and the impregnating solution the maximum corresponds more or less to the limit of dissolution of the starting material inside the pore volume of the support considered. The highest catalytic performances are obtained with the $Co_2Mo_{10}Co$ alumina based catalysts. We recently assigned the beneficial effect of this starting material to both an improvement of promoting effect, the cobalt and molybdenum being inserted in the same HPA entity, and to an increase the dispersion of the oxomolybdenum phase at high Mo loading [10]. The conversions obtained with CoMoPA catalysts are lower than those observed with $Co_2Mo_{10}CoA$ in relation to a

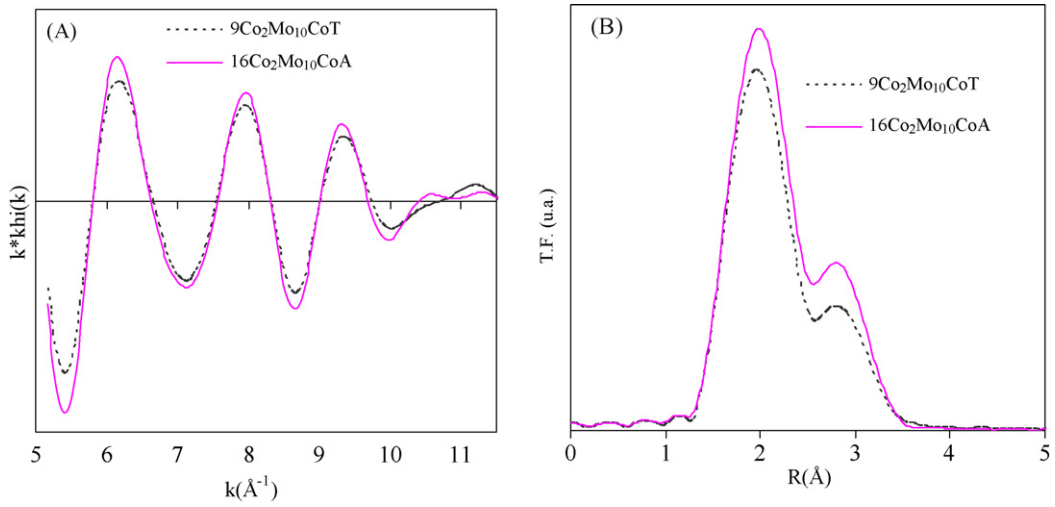

Fig. 6. EXAFS signal at the Mo K-edge (A) and Fourier transform modulus [4.18–11.58 $Å^{-1}$] (B) of sulphided $9Co_2Mo_{10}CoT$ (dotted line) and sulphided $16Co_2Mo_{10}CoA$ (full line).

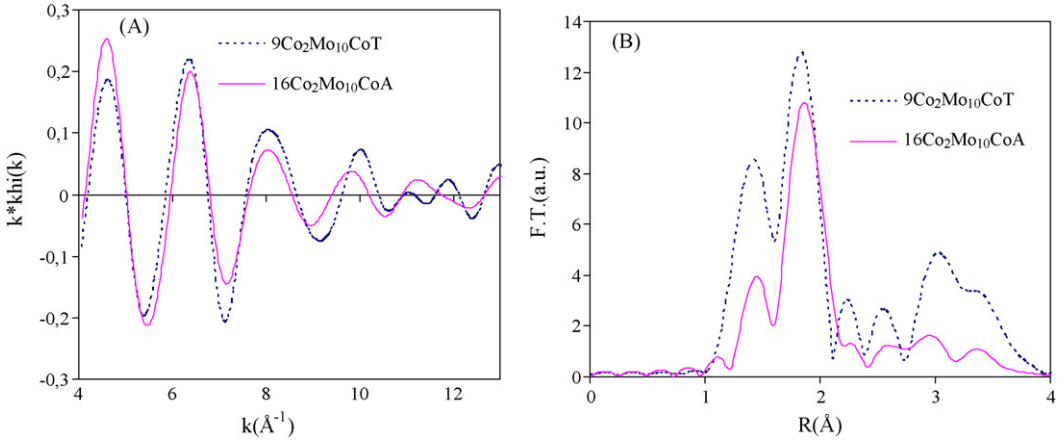

Fig. 7. EXAFS signal at the Co K-edge (A) and Fourier transform modulus [4.00–15.88 $Å^{-1}$] (B) of sulphided $9Co_2Mo_{10}CoT$ (dotted line) and sulphided $16Co_2Mo_{10}CoA$ (full line).

less efficient promoting effect. However an improvement of the dispersion is observed at high Mo loadings that explains the shift of the maximum of conversion compared to conventional CoAHM catalysts. The lower conversion at high Mo loading of CoHMA is assigned to the dispersion decrease of the oxomolybdate phase, which is due to the presence of NH_4^+ ions leading to precipitation of $AlMo_6$ ammonium salt $[AlMo_6H_6O_{24}](NH_4)_6$. TiO_2, as well as ZrO_2 based catalysts exhibit lower conversion than the alumina based ones, however the $Co_2Mo_{10}Co$ starting material appears to be the most efficient for both supports. Nevertheless, catalytic conversions measured on zirconia are inferior to those obtained on titania. Catalysts prepared from CoMoP solution give higher catalytic conversion than the conventional catalysts as already reported in literature except on TiO_2 where the performances are similar.

4. Discussion

The activity of HDS catalysts depends strongly on the exact nature of the sulphide active phase (morphology and promotion). Variation of the MoS_2 slabs stacking is observed for the various catalysts but this should not have any effect on the thiophene HDS conversion because this model reaction is not sensitive to the stacking. A HRTEM analysis also gives the same average length of the MoS_2 crystallites for example on $Co_2Mo_{10}CoA$, $Co_2Mo_{10}CoT$ and $Co_2Mo_{10}CoZ$. Moreover the XPS spectra are similar whatever the catalysts studied and do not show the existence of Co_9S_8 species in agreement with EXAFS data. This suggests that the main effect on catalytic performances is coming from the dispersion of the active elements in the oxidic precursors which also could affect the promoting effect.

The Raman study shows that on alumina the use of CoMoP impregnating solution permits to improve the dispersion at high Mo loadings, which induces an improvement of the HDS conversion by comparison to conventional catalysts. Indeed in these catalysts, the absence of counterions as ammonium prevents the precipitation of $[AlMo_6H_6O_{24}](NH_4)_6$ crystallites but it also permits a stronger interaction between the Co^{2+} and the diphosphopentamolybdate species. Both the dispersion and the promoting effect are improved, less Co atoms being lost in the alumina support. Similar effects are observed with the

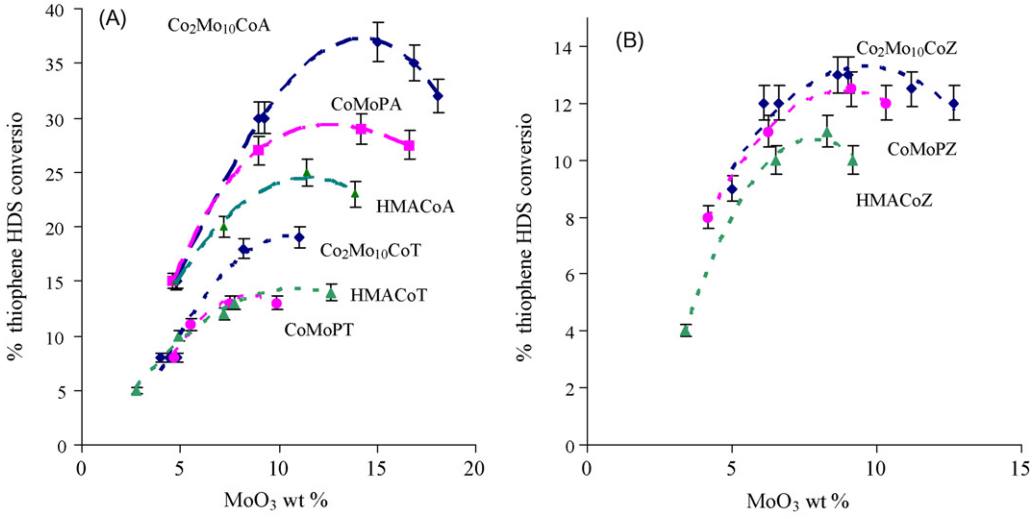

Fig. 8. Thiophene conversion vs. MoO_3 (wt.%) for Al_2O_3 and TiO_2 supported catalysts (A) and ZrO_2 supported catalysts (B).

$Co_2Mo_{10}Co$ starting impregnating solution. We have reported in the experimental part that the solubilities for AHM and $[Co_2Mo_{10}O_{38}H_4]^{6-}$ HPA are rather similar. So the determining factor for limiting the dispersion at high Mo loading on conventional preparation is the formation of $[AlMo_6O_{24}H_6(NH_4)_3]$ which solubility is low; the precipitation from the 6molybdoaluminate anion being due to the presence of of NH_4^+ ions in the impregnating solution. In $[Co_2Mo_{10}O_{38}H_4]^{6-}$ HPA, it can be considered that the Co atoms are directly chelated by the molybdate ligands. These entities are preserved upon deposition which also participates to the improvement of the promoting effect according the van Veen's principle.

The same comparison performed on the TiO_2 supported catalysts does not point out such differences between the uses of the three impregnating solutions. Indeed Raman spectroscopic characterizations showed that the dispersion is optimal whatever the starting solution and the HDS conversion of the CoMoPT and AHMCoT catalysts are quite similar, which suggests that the presence of P has neither effect on the dispersion nor on the catalytic activity. Moreover, the absence of ammonium counter ions has no effect, which also suggests the absence of any dissolution–precipitation phenomenon on TiO_2. Thus with the titania support the higher conversion of the $Co_2Mo_{10}Co$ based catalyst can only be assigned to the improvement of the promoting effect induced by the use of this HPA despite its non preservation on the support after maturation.

Zirconia supported catalysts are less efficient than the TiO_2 ones at similar Mo loading but the conversion of the AHMCoZ catalyst is lower than the CoMoP one. This can be explained by the lower dispersion of the oxomolybdate entities on the CoAHM oxidic precursor as bulk $CoMoO_4$ and MoO_3 oxides were identified by Raman spectroscopy. On ZrO_2, the use of CoMoP solution increases the dispersion as observed on alumina. But here also the higher conversion of the $Co_2Mo_{10}Co$ based catalyst is assigned to the improvement of the promoting effect (by comparison with CoMoPZ) and of the Mo dispersion at high Mo loading (by comparison with AHMCOZ).

This study of TiO_2 and ZrO_2 HPA based catalysts points out the beneficial use of the $Co_2Mo_{10}O_{38}H_4^{6-}$ species. Only the particular structure of the later HPA where Mo and Co are inserted in the same entity can explain the highest activity in thiophene HDS.

Thus whatever the support used, the heteropolycompound $Co_3[Co_2Mo_{10}O_{38}H_4]$ appears as the starting material that induces on improvement of the thiophene HDS conversion thanks to the improvement of the dispersion in the oxidic state and/or of the promotion in the sulphided state. The best activities (obtained with $Co_2Mo_{10}Co$ impregnating solution) are respectively 4.09×10^{-1}, 3.65×10^{-1} and 2.40×10^{-1} thiophene mol (Mo mol s)$^{-1}$ for Al_2O_3, TiO_2 and ZrO_2 supported catalyst and are obtained for different Mo loadings but corresponding to similar Mo density (number of Mo per nm^2—dMo), i.e. around 3.4 molybdenum atoms nm^{-2}. Even if the intrinsic activity is lower on titania than on alumina, the high density of TiO_2 (≈1.5 superior than the alumina one) would lead to an important volumic HDS activity making this support attractive if its textural properties (SSA and pore volume) can be still improved.

5. Conclusion

In this work, alumina, titania and zirconia supported HDS catalysts have been studied. A comparison between three methods of preparation of CoMo catalysts has been undertaken through impregnation with solutions containing AHM or the well-defined heteropolyanions $P_2Mo_5O_{23}^{6-}$ and $Co_2Mo_{10}O_{38}H_4^{6-}$, the Co/Mo ratio being fixed at 0.5. Thiophene HDS conversions show that the best catalytic results are obtained on alumina and with the use of $Co_2Mo_{10}Co$ solution as reported in the literature. The conversions obtained on titania (or zirconia) are lower but the $Co_2Mo_{10}Co$ based catalysts are always the most efficient. This HPA where Mo and Co are in the same entity permits to have the best promoting effect by the cobalt atoms. On zirconia, a better dispersion is also obtained with the use of the two HPA, MoO_3 and $CoMoO_4$ phases being characterized by Raman analysis in conventional supported ZrO_2 oxidic precursor. However in this work the same sulphidation conditions were applied, which could have a levelling effect. A study of the genesis of the sulphided phase of these various solids is therefore now under progress.

References

[1] N.Y. Topsoe, H. Topsoe, J. Catal. 75 (1982) 354.
[2] A. Spozhakina, S. Damyanova, V. Sharkova, D. Shopov, Proc. VI Int. Symp. Heterogeneous Catalysis Sofia, 1987, part I 503.
[3] W.C. Cheng, N.P. Luthra, J. Catal. 109 (1988) 163.
[4] A.M. Maitra, N.W. Cant, Appl. Catal. 48 (1989) 187.
[5] C.I. Cabello, I.L. Botto, H. Thomas, Appl. Catal. A 197 (2000) 79.
[6] C.I. Cabello, F. Cabrerizo, A. Alvarez, H. Thomas, J. Mol. Catal. 186 (1–2) (2002) 89.
[7] J.A.R. Van Veen, P.A.J.M. Hendriks, R.R. Andrea, E.J.G.M. Romers, A.E. Wilson, J. Phys. Chem. 94 (1990) 5282.
[8] C. Martin, C. Lamonier, M. Fournier, O. Mentré, V. Harlé, D. Guillaume, E. Payen, Inorg. Chem. 43 (2004) 4636.
[9] C. Martin, C. Lamonier, M. Fournier, O. Mentré, V. Harlé, D. Guillaume, E. Payen, Chem. Mater. 17 (2005) 4438.
[10] C. Lamonier, C. Martin, J. Mazurelle, V. Harlé, D. Guillaume, E. Payen, Appl. Catal. B: Environ. 70 (2007) 548.
[11] J.A.R. van Veen, P.A.J.M. Hendriks, R.R. Andrea, E.J.G.M. Romers, A.E. Wilson, J. Phys. Chem. 94 (1990) 5282.
[12] A. Griboval, P. Blanchard, E. Payen, M. Fournier, J.L. Dubois, Catal. Today 45 (1998) 277.
[13] A. Griboval, P. Blanchard, L. Gengembre, E. Payen, M. Fournier, J.L. Dubois, J.R. Bernard, J. Catal. 188 (1999) 102.
[14] V. Harlé, J.P. Deloume, L. Mosoni, B. Durand, M. Vrinat, M. Breysse, Eur. J. Solid State Inorg. Chem. 31 (1994) 197.
[15] T. Ono, Y. Ohguchi, O. Togari, Stu. Surf. Sci. Catal. 16 (1983) 631.
[16] J. Ramirez, I. Ruiz-Ramirez, L. Cedeno, V. Harlé, M. Vrinat, M. Breysse, Appl. Catal. A 93 (1993) 163.
[17] Y. Okamoto, A. Maezawa, T. Imanaka, J. Catal. 120 (1989) 29.
[18] D.H. Wang, E.W. Qian, A. Ishibara, T. Kabe, J. Catal. 203 (2001) 322.
[19] H. Shimada, Catal. Today 86 (2003) 17.
[20] M. Vrinat, M. Breysse, C. Geantet, J. Ramirez, F. Massoth, Catal. Lett. 26 (1994) 25.
[21] C. Arrouvel, M. Breysse, H. Toulhoat, P. Raybaud, J. Catal. 232 (2005) 161.
[22] D. Costa, C. Arrouvel, M. Breysse, H. Toulhoat, P. Raybaub, J. Catal. 246 (2007) 325.

[23] G. Plazenet, S. Cristol, J.F. Paul, E. Payen, J. Lynch, Phys. Chem. Chem. Phys. 3 (2001) 246.
[24] P.W. de Bont, M.J. Vissenberg, E.J.M. Hensen, V.H.J. de Beer, J.A.R. van Veen, R.A. van Santen, A.M. van der Kraan, Appl. Catal. A: Gen. 236 (2002) 205.
[25] B.R.G. Lelived, J.A.J. van Dillen, J.W. Geus, D.C. Koningberger, M. de Boer, J. Phys. Chem. B 101 (1997) 11160.
[26] J.T. Miller, C.L. Marshall, A.J. Kropf, J. Catal. 202 (2001) 89.
[27] Y. Okamoto, Catal. Today 39 (1997) 45.